On the Outage Performance of Reconfigurable Intelligent Surface-Assisted UAV Communications

Mohammad Abualhayja'a, Anthony Centeno, Lina Mohjazi, Qammer H Abbasi, and Muhammad Ali Imran

James Watt School of Engineering, University of Glasgow, Glasgow, UK

Email: m.abualhayja'a.1@research.gla.ac.uk,

{Anthony.Centeno, Lina.Mohjazi, qammer.abbasi, Muhammad.Imran}@glasgow.ac.uk

Abstract—Unmanned aerial vehicles (UAVs) and reconfigurable intelligent surfaces (RISs) are expected to be widely used in future wireless communication networks to improve the spectrum and energy efficiency. In this paper, RIS-assisted UAV communication systems are studied and analysed by developing a comprehensive mathematical framework for examining their outage performance. In order to study the effect of the RIS on the UAV communications, two system scenarios are considered: in the first scenario, the UAV acts as an aerial base station (BS) serving a ground user to offload the terrestrial network, and in the second system, the UAV acts as an aerial user served by a terrestrial BS. We present channel models considering the UAV's unique characteristics, propose a closed-form approximation for the signal-to-noise-ratio (SNR) distribution, and derive an analytical expression for the relevant outage probability. Results show that RIS can significantly improve the performance of UAV communication systems by introducing energy efficient and reliable links. This opens the door for UAV networks, which are highly scalable, adaptable, and robust to environmental changes. Furthermore, the results show that the UAV position and altitude optimisation significantly affects the outage performance.

Index Terms—Unmanned aerial vehicle, reconfigurable intelligent surfaces, Rician fading, outage probability.

I. INTRODUCTION

Unmanned aerial vehicles (UAVs) are playing an increasingly significant role in the future wireless networks with several potential applications due to their unique mobility and flexibility characteristics. UAVs may be utilised as airborne communication platforms to improve the wireless network coverage, capacity, reliability, and energy efficiency. Due to UAVs' high mobility, they can be flexibly deployed to enhance the communication quality, while conventional terrestrial base station (BS) only serves the ground users in a fixed area. On the other hand, they can function as new aerial user equipment (UE) terminals in the cellular network serving various applications, ranging from data collection to item delivery [1]–[4]. Hence, based on their functionality, there are two major paradigms for integrating UAVs into cellular networks. The first is the UAV-aided communications, in which UAVs serve as aerial communication platforms or a BS. The second is cellular-connected UAV paradigm, where UAVs operate as aerial users/terminals in a cellular network to serve different applications.

The explosive growth in the number of deployed UAV nodes implies the need to reshape the traditional terrestrial networks to address several challenges, such as dynamic placement,

high mobility, and other challenges related to the existing terrestrial networks planning [5]. For instance, the optimal three-dimensional (3D) placement is one of the most critical aspects of UAV-assisted communications [6], [7]. However, due to their high mobility, it is a challenging task to achieve optimal UAVs 3D deployment, especially in multi-UAVs deployment scenarios. In fact, there are multiple factors that must be considered such as inter-cell interference, energy and spectrum constraints, ground users' geographical distribution, traffic demands, and the varying air-to-ground (A2G) channel characteristics [6]. Moreover, due to their relatively high altitude, UAVs will receive line-of-sight (LoS) signals from multiple terrestrial BSs. Field trials show that the number of detectable cells increases as the UAV altitude increases. Hence, the interference in cellular-connected UAV systems significantly increases at high UAV altitude causing low signal-to-interference-and-noise-ratio (SINR) [8]. Moreover, due to their fast movement, cellular-connected UAVs introduce new challenges in terms of mobility management and the essential need to ultra-reliable low latency communications (URLLC) navigation and control links [2], [8].

Hence, a reliable and improved coverage is essential to meet the needs of UAV-enabled wireless communication networks. To this effect, reconfigurable intelligent surfaces (RISs) has been identified as a revolutionary technology that can potentially assist UAV communications and enhance the network performance in terms of spectrum and energy efficiency [9], [10]. RIS has recently attracted both academics and industry as a low-cost, smart, and energy-saving solution for enhancing wireless network spectrum efficiency and coverage. This is due to the RISs ability to control the wireless environment by creating virtual LoS links between the communication nodes [11]. RISs can be implemented to support A2G links between the aerial platforms and ground users to maximise the UAV coverage area and increase the transmit power efficiency [9], [10]. RISs can also help to solve challenges related to the UAV optimal path planning such as intercell interference, backhauling, and other physical constraints i.e., UAV dynamics, flying speed, and acceleration. Furthermore, as RISs are deployed for local coverage only, their operating ranges are usually much shorter than those of active BSs/relays, which makes it easier to practically deploy RISs without interfering each other. Hence, RISs can also overcome the SINR degradation caused by the severe interference at cellular-connected UAV networks,

this will be reflected on the network performance in terms of radio-link-failure (RLF) and reduces unnecessary handovers (HOs) caused by high numbers of detected cells. The RIS-aided UAV communication shows an improved performance in terms of power efficiency, coverage, capacity, and reliability [9], [10], [12]–[14].

Use cases and performance analysis of RIS-assisted UAV communication systems have not been thoroughly explored in the literature. However, recently, noticeable research efforts proposed RIS-assisted UAV as a promising solution to extend wireless networks coverage and enhance their performance. In [9], the authors proposed an algorithm to maximise the achievable rate of a UAV BS serving a ground user by jointly optimising the RIS passive beamforming matrix and the UAV trajectory. The work carried out in [10] considers a system with multiple RISs supporting a UAV BS to maximise the received power by a ground user. In [12], the authors proposed a UAV-enabled solution, where the UAV is equipped with an RIS and acts as a passive relay between a ground BS and ground UEs to maximise the secure energy efficiency against an eavesdropper by optimising the UAV trajectory, RIS passive beamforming, user association, and transmitted power. The work in [13] proposed a performance analysis of a RIS-assisted UAV communication system, where a UAV acts as a relay and RIS is deployed to support the link from BS to the UAV. Their results show that RIS deployment can enhance the system performance in terms of reliability, average bit error rate (BER), and average capacity. In our previous work in [15], we offered a comparison between the performance of RIS and relay- assisted UAV communications. Results show that the RIS should be equipped with more than one hundred reflecting elements to match up to a single DF relay performance in terms of the achievable rate. It was also observed that an RIS with a sufficiently high number of elements attains a better performance, in terms of power requirements, in the case of high UAV altitudes.

In this work, to develop a better understanding of net-work the UAV performance and the outage probability for RIS-assisted UAV communications is studied and analysed considering both UAV integration paradigms, (i) UAV-aided communications: UAV aerial BS serving a ground user, and an RIS supports A2G communication, (ii) cellular connected-UAV system: where UAV acts as an aerial UE served by a ground BS and an RIS supports G2A communication. Since UAVs usually have high LoS probability, which is also related to the UAV elevation angle, Rician fading channels are assumed between the UAV and the RIS in both setups, and channel parameters are defined taking into consideration the special characteristics of the UAV communications, which makes it different from the work represented in [16]. Motivated by UAV special channel characteristics, optimal altitude of the UAV is also observed for performance enhancement. The specific contributions of this work can be summarised as follows:

- Characterise the outage probability of RIS-assisted UAV communications for both of the UAV deployment
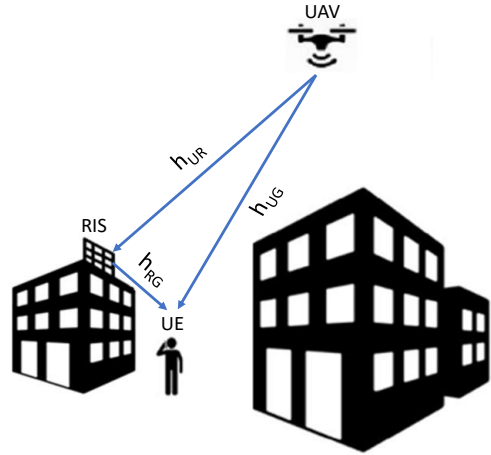
Figure 1: RIS-assisted UAV-aided communications.

paradigms, taking into account the special characteristics of the UAV communications.
- Derive approximate expressions for the proposed system models outage probability. The analytical expressions are validated by comparing to results of Monte Carlo simulations.
- Offer asymptotic analysis for high SNR regime.
- Study the effect of the optimal UAV altitude and the number of RIS elements for an enhanced performance.

The rest of the paper is structured as follows. Section II describes the system model of the proposed RIS-assisted UAV communications systems. In Section III, the SNR outage probability is characterised for both systems scenarios. Then, the numerical results are presented in Section IV and the conclusion is offered in Section V.

II. SYSTEM MODEL

In this section, we describe the proposed RIS-assisted UAV models. Two models are considered, UAV-aided and cellular-connected UAV communications.

A. RIS to support A2G communications

We consider a communication network scenario where a UAV acts as an aerial BS serving ground user equipment UE, and RIS is deployed on wall of a building to assist the link between UAV and a ground user, as depicted in Fig. 1. The RIS is equipped with a uniform linear array (ULA) of M reflecting elements. The signal received by the UE can be written as

$$y_1 = \left(h_{UG} + h_{UR}^H \Theta h_{RG} \right) x_1 + n_1, \qquad (1)$$

where h_{UG}, h_{UR}, and h_{RG} are the channel gains from the UAV-UE, UAV-RIS, and RIS-UE links, respectively. $\Theta = \text{diag} \left\{ e^{j\theta_1}, e^{j\theta_2}, \ldots, e^{j\theta_M} \right\}$ is the RIS diagonal phase-shift matrix, x_1 is the transmitted signal from the UAV, and $n_1 \sim \mathcal{CN}(0, N_0)$ is the additive white Gaussian noise (AWGN) at the UE with zero mean and N_0 variance.

The UAV trajectory is assumed to be optimised in order to achieve LoS connection with the ground user. The channel gain for UAV-UE link can be expressed as

$$h_{UG} = \sqrt{\rho d_{UG}^{-2}}, \qquad (2)$$

where ρ is the path loss at the reference distance of 1m, and d_{UG} is the distance between the UAV and the UE.

UAVs usually fly at relatively high altitudes and RISs are commonly placed on the facade of a building [9]. This will increase the probability to have a LoS link between the RIS and the UAV. In additional to the LoS component, the UAV-RIS link is assumed to have scattered multi-path components. Hence, the channel gain for UAV-RIS link can be modelled by a Rician distribution, and can be expressed as

$$h_{UR} = \sqrt{\rho d_{UR}^{-\alpha}} \left(\sqrt{\frac{K_1}{K_1+1}} \bar{h}_{UR}^{LoS} + \sqrt{\frac{1}{K_1+1}} \widetilde{h}_{UR}^{NLoS} \right), \qquad (3)$$

where d_{UR} is the distance between the UAV and the RIS, α is the path loss exponent, K_1 is the Rice factor, and $\widetilde{h}_{RG}^{NLoS}$ represents the random scattering non-line-of-sight (NLoS) component, modelled by a zero-mean and unit-variance complex Gaussian random variable. The deterministic LoS component of the UAV-RIS link is represented by the RIS array response as

$$\bar{h}_{UR}^{LoS} = \left[1, e^{-j\frac{2\pi}{\lambda}d\phi_{UR}}, \dots, e^{-j\frac{2\pi}{\lambda}(M-1)d\phi_{UR}} \right]^T, \qquad (4)$$

where ϕ_{UR} is the angle between the UAV and the RIS, and λ is the wave length.

RIS achieves the maximum channel gain when it is close to the source or to the destination [17]. Hence, the RIS will be placed close to the serving area, which can also guarantees a LoS link between the RIS and the ground user. The channel gain for RIS-UE link can be modelled as

$$h_{RG} = \sqrt{\rho d_{RG}^{-2}} \left[1, e^{-j\frac{2\pi}{\lambda}d\phi_{RG}}, \dots, e^{-j\frac{2\pi}{\lambda}(M-1)d\phi_{RG}} \right]^T, \qquad (5)$$

where d_{RG} is the distance between the RIS and the UE.

As a result, the SNR at the UE can be written as

$$\gamma_1 = \frac{P_1 \left| h_{UG} + h_{UR}^H \Theta h_{RG} \right|^2}{N_0}. \qquad (6)$$

From [9], the maximum instantaneous SNR at the UE can be achieved by the phase alignment of the signals at the user, therefore, (6) can be rewritten as

$$\gamma_1 = \frac{P_1 \left(|h_{UG}| + \sum_{i=1}^{M} |h_{UR,i}| |h_{RG,i}| \right)^2}{N_0}. \qquad (7)$$

B. RIS to support G2A communications

As shown in Fig. 2, for the cellular-connected UAV scenario, we consider a system setup where a UAV acts as an
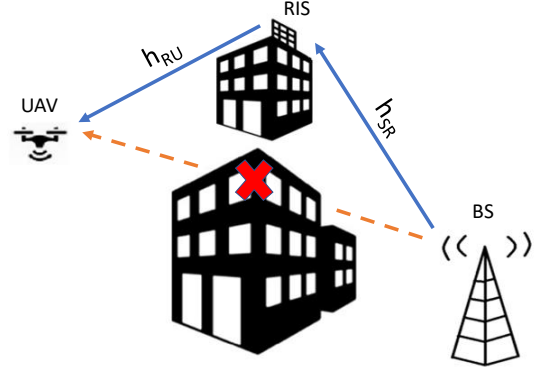
Figure 2: RIS-assisted cellular-connected UAV communications.

aerial user served by a single antenna terrestrial BS, and RIS is deployed on a building to assist the link between the terrestrial BS and the UAV. The RIS is equipped with a ULA of M reflecting elements. The received signal at the UAV can be written as

$$y_2 = \left(h_{SR}^H \Theta h_{RU} \right) x_2 + n_2, \qquad (8)$$

where h_{SR} and h_{RU} are the channel gains for the BS-RIS and RIS-UAV links, respectively. $\Theta = \alpha \, \text{diag} \left\{ e^{j\theta_1}, e^{j\theta_2}, \dots, e^{j\theta_M} \right\}$ is the RIS diagonal phase-shift matrix, x_2 is the transmitted signal from the BS, and $n_2 \sim \mathcal{CN}(0, N_0)$ is the AWGN at the ground user with zero mean and N_0 variance.

In additional to the LoS component, the links comprise scattered multi-path components. Hence, the channel gains can be modelled by Rician fading as

$$h_i = \sqrt{\rho d_i^{-\varepsilon_i}} \left(\sqrt{\frac{K_i}{K_i+1}} \bar{h}_i^{LoS} + \sqrt{\frac{1}{K_i+1}} \widetilde{h}_i^{NLoS} \right), \qquad (9)$$

where $i \in (SR, RU)$, d_i is the distance between nodes, ε_i is the path loss exponent, and K_i is the Rician factor.

As a result, the SNR at the UE can be written as

$$\gamma_2 = \frac{P_2 \left| h_{UR}^H \Theta h_{RG} \right|^2}{N_0}. \qquad (10)$$

Hence, the maximum instantaneous SNR at the UE can be expressed as

$$\gamma_2 = \frac{P_2 \left(\sum_{i=1}^{M} |h_{UR,i}| |h_{RG,i}| \right)^2}{N_0}, \qquad (11)$$

III. PERFORMANCE ANALYSIS

In this section, we characterise the performance of the proposed system in terms of the outage probability.

A. RIS to support A2G communications

The outage probability represents the cumulative distribution function (CDF) of the SNR evaluated at the desired threshold SNR, γ_{th}. Using (7), the SNR for the first scenario can be re-written as

$$\gamma_1 = \frac{P_1 \left(|h_{UG}| + \sum_{i=1}^{M} |h_{UR,i}| |h_{RG,i}| \right)^2}{N_0} = \overline{\gamma}_1 R^2, \quad (12)$$

where $\overline{\gamma}_1 = \frac{P_1}{N_0}$ is the average SNR, and

$$R = |h_{UG}| + \sum_{i=1}^{M} |h_{UR,i}| |h_{RG,i}|. \quad (13)$$

The outage probability can be expressed as

$$P_{\text{out1}} = P_r \left(\gamma_1 \leq \gamma_{th} \right) = P_r \left(R \leq \sqrt{\frac{\gamma_{th}}{\overline{\gamma}_1}} \right), \quad (14)$$

By substituting (13) in (14), the outage probability can be written as

$$P_{\text{out1}} = P_r \left(\sum_{i=1}^{M} |h_{UR,i}| \leq \frac{\sqrt{\frac{\gamma_{th}}{\overline{\gamma}_1}} - |h_{UG}|}{|h_{RG}|} \right). \quad (15)$$

The term $\sum_{i=1}^{M} |h_{UR,i}|$ involves the summation of M independent and identically distributed (i.i.d.) Rician random variables. However, to the best of our knowledge, a closed-form expression for this summation does not exist in the literature and its derivation is mathematically intractable. Hence, we resort to deriving a simple and accurate closed-form approximation for this sum.

The authors of [16], proposed a closed-form approximation to the sum of Rician distributions based on modifying the sum distribution of the squared Rician random variables. The CDF of the sum of Rician random variables can be presented as

$$F_M(t) = 1 - Q_M \left(\frac{b}{c_1}, \frac{t}{c_2} \right), \quad (16)$$

where $Q_\zeta(.,.)$ is the generalised Marcum Q-function with parameter ζ [18], c_1 and c_2 are constants, $b = \sqrt{\frac{MK\Omega}{K+1}}$, and $t = \frac{r}{\sqrt{M}}$ is the normalised argument.

Thus, the outage probability can be written as

$$P_{out1} = 1 - Q_M \left(\frac{b}{c_1}, \frac{1}{c_2} \left(\frac{\sqrt{\frac{\gamma_{th}}{\overline{\gamma}_1}} - \sqrt{\rho d_{UG}^{-2}}}{\sqrt{\rho d_{RG}^{-2}} \sqrt{\rho d_{UR}^{-\alpha}}} \right) \right). \quad (17)$$

For a better understanding to the system performance in terms of the achievable diversity order and the coding gain, the asymptotic or high SNR analysis is derived next. From [19], the generalised Marcum-Q function has the following asymptotic form

$$Q_M(x, y) \sim \sum_{n=0}^{\infty} \psi_n, \quad (18)$$

where, ψ_n can be written as

$$\psi_n = \frac{\mu^M}{2\sqrt{2\pi}} (-1)^n \left[A_n(M-1) - \frac{1}{\mu} A_n(M) \right] \nu_n, \quad (19)$$

where, $\mu = \sqrt{y/x}$, $\nu_n = \left[\frac{(y-x)^2}{2xy} \right]^{n-\frac{1}{2}} \Gamma \left(\frac{1}{2} - n, \frac{(y-x)^2}{2} \right)$, $A_n(M) = \frac{2^{-n} \Gamma \left(\frac{1}{2} + M + n \right)}{n! \Gamma \left(\frac{1}{2} + M - n \right)}$, and $\Gamma(.)$ is the Gamma function.

As $\overline{\gamma} \to \infty$ the first term in the summation in (18) becomes dominating over the other terms. Assuming $y > x$, the first term of the asymptotic approximation in (18) can be written as [19]

$$Q_M(x, y) \sim \psi_0 = \left(\frac{y}{x} \right)^{M-\frac{1}{2}} Q(y-x). \quad (20)$$

where $Q(.)$ is the Gaussian Q function.

Using (17) and (20), the asymptotic outage probability can be written as

$$\rho_{\text{out 1}}^{\infty} \simeq 1 - \left(\frac{\frac{1}{c_2} \left(\frac{\sqrt{\frac{\gamma_1}{\gamma_{hh}}} - \sqrt{\rho d_{UG}^2}}{\sqrt{\rho d_{RG}^2} \sqrt{\rho d_{UR}^\alpha}} \right)}{\frac{b}{c_1}} \right)^{M-\frac{1}{2}}$$
$$\times Q \left(\frac{1}{c_2} \left(\frac{\sqrt{\frac{\gamma_{hh}}{\gamma_1}} - \sqrt{\rho d_{UG}^{-2}}}{\sqrt{\rho d_{RG}^{-2}} \sqrt{\rho d_{UR}^{-\alpha}}} \right) - \frac{b}{c_1} \right). \quad (21)$$

B. RIS to support G2A communications

From (11) the SNR for the second scenario can be re-written as

$$\gamma_2 = \frac{P_2 \left(\sum_{i=1}^{M} |h_{UR,i}| |h_{RG,i}| \right)^2}{N_0} = \overline{\gamma}_2 X^2, \quad (22)$$

where $\overline{\gamma}_2 = \frac{P_2}{N_0}$ is the average SNR, and the term $X = \sum_{i=1}^{M} |h_{UR,i}| |h_{RG,i}|$ is the sum of the product of two Rician random variables. The authors in [20] proposed a closed-form approximation for this summation.

Using (18) and [17, Eq. (7)], the outage probability can be approximated as:

$$P_{out2} \simeq \frac{\gamma \left(e+1, \frac{\sqrt{\gamma_{th}}}{v\sqrt{\overline{\gamma}_2}} \right)}{\Gamma(e+1)}, \quad (23)$$

where, $\gamma(\cdot, \cdot)$ is the lower incomplete gamma function, e and v are parameters related to the mean and variance of X.

Similarly for this setup, from (23) and [17, Eq. (14)] the asymptotic outage probability can be written as

$$P_{\text{out2}}^{\infty} \simeq \left[\frac{v^2}{\gamma_{\text{out}} \left[(e+1)! \right]^{-\frac{2}{(e+1)}}} \bar{\gamma} \right]^{-\frac{(e+1)}{2}}. \qquad (24)$$

Due to the special the characteristics of the UAV channels, both the Rice factor and the path loss exponent depend on the LoS probability. They can be expressed as a function of θ, the angle between the UAV and the communication node as [21], [22]

$$K(\theta) = A_K e^{B_K \theta}, \qquad (25)$$

and,

$$\eta(\theta) = A_\eta P_{\text{LoS}}(\theta) + B_\eta. \qquad (26)$$

where $\eta \in (\alpha, \varepsilon_{RU})$, $P_{LoS}(\theta) = \frac{1}{1+\beta e^{-b(\theta-a)}}$ is the LoS probability, A_i, B_i, $i \in (K, \eta)$ are parameters that depend on the environment and the transmission frequency, and β, a, b are environment variables [19].

IV. NUMERICAL AND SIMULATION RESULTS

In this section, we present numerical results to verify our analysis and to obtain insights into the effect of the RIS size and the UAV positioning (altitude) on the system's perform- ance. The simulation parameters are set as follows: $\rho = 20$ dB, $\varepsilon_{RU} = 2.8$, $K(0) = 5$ dB, $k(\pi/2) = 15$, $A_1 = 1.5$, and $B_1 = 3.5$. Also, unless otherwise stated, $P_1 = 0.01$ W, and $P_2 = 0.1$ W, it is worth mentioning that the transmit power is selected for the aerial BS to be lower than the terrestrial BS due to the power limitations on the UAV.

Fig. 3 and Fig. 4 represent the outage probability as a function of the UAV height for the UAV-aided communica- tion and the cellular-connected UAV communication systems, respectively. Both figures show that the analytical results are consistent with the simulations. It can be observed that the outage probability performance of the two considered scenarios experience a significant improvement as the number of RIS elements increases. Thus, a RIS with a sufficiently high number of elements can maintain reliable connections between aerial and terrestrial nodes. Moreover, it can be also noticed that the performance improves as the UAV height increases, since both the Rician factor and the path loss exponent are affected by the LoS probability, which becomes higher as the elevation angle of the UAV increases, or in other words as the UAV flies at relatively high altitudes. However, the performance degrades again when the UAV elevation angle variations become insignificant and the path loss starts to increase due to the increased UAV altitude. It is also worth noting that despite the fact that a LoS link exists between the UAV and the ground user, as shown in Fig. (3), the RIS significantly affects the performance of the system, and even a small increase in the number of the RIS elements can noticeably improve the system performance.

Figs. 5 and 6 examine the outage probability performance of the A2G and G2A setups, respectively, as a function of the transmit SNR for different numbers of RIS elements. The UAV height is selected based on the results presented in Fig.
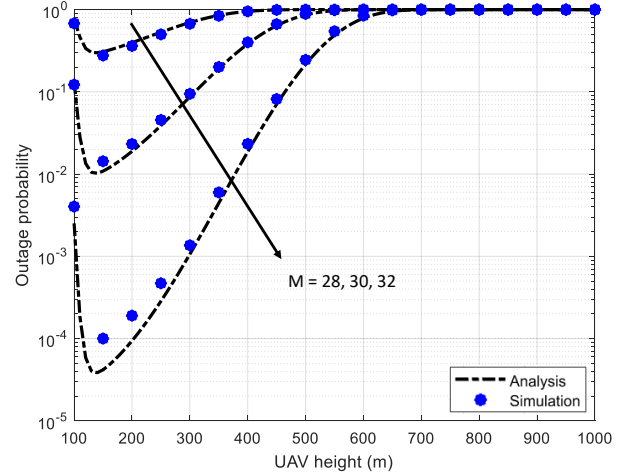
Figure 3: P_{out} versus UAV height for different number of RIS elements for RIS-assisted UAV communication (A2G).
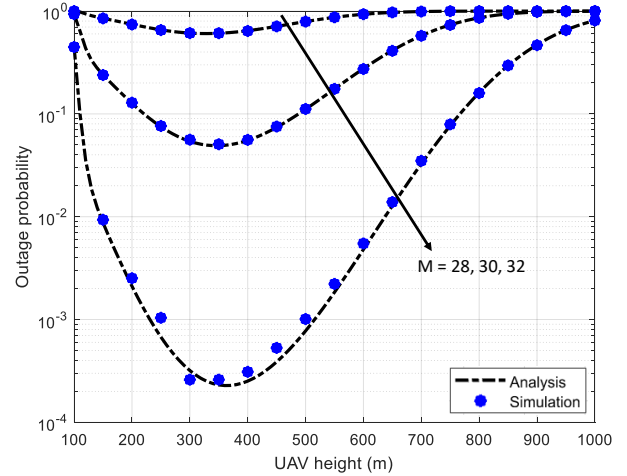
Figure 4: P_{out} versus UAV height for different number of RIS elements for RIS-assisted UAV communication (G2A).

3 and Fig. 4 to achieve the maximum performance, where the UAV heights are set as 130 m for the first systems and 350 m for the cellular-connected UAV system. Again, the analytical results are consistent with the simulations in both scenarios. As expected, the RIS with a larger number of elements achieves an improved performance. It can be also observed that the performance of the system with a larger RIS is similar to the high SNR performance of the systems with a lower number of RIS elements. For instance, in Fig. 6, the RIS with 24 elements achieves a similar outage performance at transmit SNR of 76 dB as the 20 elements RIS at SNR of 80 dB. This will result in maintaining the quality of communication links by providing energy efficient and reliable connections for different propagation environment and users traffic demands. Furthermore, in the case of cellular-connected UAVs and the expected multiple cell detection, increasing the number of the RIS elements can overcome the SNR degradation problem
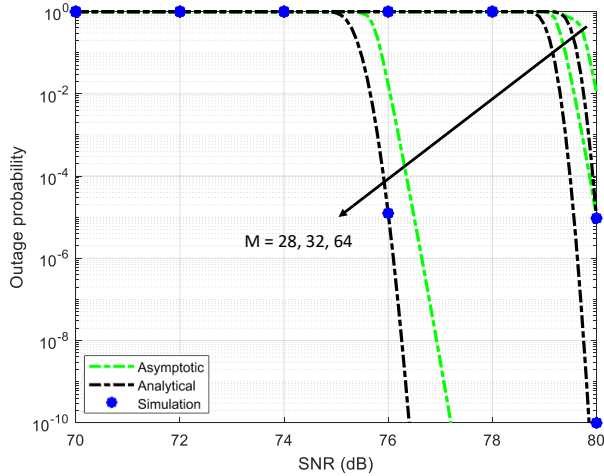
Figure 5: P_{out} versus SNR for different number of RIS elements for RIS-assisted UAV communication (A2G).
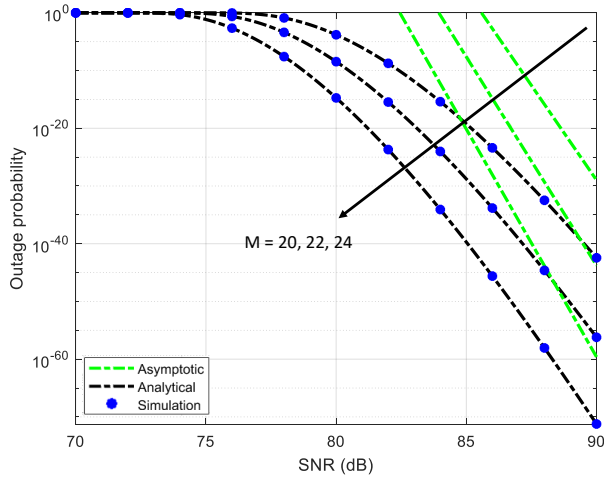
Figure 6: P_{out} versus SNR for different number of RIS elements for RIS-assisted UAV communication (G2A).

which will reduce the RLFs caused by interference. This improvement will also reflected on the mobility management and reduces any unnecessary HOs.

V. CONCLUSION

In this work, a theoretical framework to analyse the performance of RIS-assisted UAV communications was proposed. We presented the system and channel models taking into consideration the UAV special characteristics. Closed-form approximations for the SNR distributions and the outage probability were derived for two different scenarios, namely, RIS-assited UAV-aided communications and RIS-assisted cellular-connected UAV communications. These expressions are exploited to evaluate the outage performance of the proposed systems. It is observed that the analytical results are almost matching with the simulation results. Moreover, the results showed that the RIS can significantly improve the perform-

ance of UAV communication systems by maintaining reliable connections. It can be also noticed that the UAV achieves an improved performance as the UAV altitudes increases due to the high line of sight probability, which improves the link reliability.

REFERENCES

[1] N.-N. Dao *et al.*, "Survey on Aerial Radio Access Networks: Toward a Comprehensive 6G Access Infrastructure," *IEEE Commun. Surveys Tuts.*, vol. 23, no. 2, pp. 1193–1225, 2021.

[2] M. Mozaffari *et al.*, "A Tutorial on UAVs for Wireless Networks: Applications, Challenges, and Open Problems," *IEEE Commun. Surveys Tuts.*, vol. 21, no. 3, pp. 2334–2360, 2019.

[3] Y. Zeng, Q. Wu, and R. Zhang, "Accessing From The Sky: A Tutorial on UAV Communications for 5G and Beyond," *Proc. IEEE Proc.*, vol. 107, no. 12, pp. 2327–2375, 2019.

[4] B. Li, Z. Fei, and Y. Zhang, "UAV Communications for 5G and Beyond: Recent Advances and Future Trends," *IEEE Internet Things J.*, vol. 6, no. 2, pp. 2241–2263, 2018.

[5] Y. Zeng, J. Lyu, and R. Zhang, "Cellular-Connected UAV: Potential, Challenges, and Promising Technologies," *IEEE Wirel. Commun.*, vol. 26, no. 1, pp. 120–127, 2018.

[6] A. A. Khuwaja *et al.*, "A survey of channel modeling for uav communications," *IEEE Commun. Surveys Tuts.*, vol. 20, no. 4, pp. 2804–2821, 2018.

[7] M. Alzenad, A. El-Keyi, F. Lagum, and H. Yanikomeroglu, "3-d placement of an unmanned aerial vehicle base station (uav-bs) for energy-efficient maximal coverage," *IEEE Wireless Commun. Lett.*, vol. 6, no. 4, pp. 434–437, 2017.

[8] 3GPP, "Enhanced LTE Support for Aerial Vehicles," *Technical report (TR) 36.777, 3rd Generation Partnership Project (3GPP)*, 2018.

[9] S. Li *et al.*, "Reconfigurable Intelligent Surface Assisted UAV Communication: Joint Trajectory Design and Passive Beamforming," *IEEE Wireless Commun. Lett.*, vol. 9, no. 5, pp. 716–720, 2020.

[10] L. Ge *et al.*, "Joint Beamforming and Trajectory Optimization for Intelligent Reflecting Surfaces-Assisted UAV Communications," *IEEE Access*, vol. 8, pp. 78 702–78 712, 2020.

[11] E. Basar *et al.*, "Wireless communications through reconfigurable intelligent surfaces," *IEEE access*, vol. 7, pp. 116 753–116 773, 2019.

[12] H. Long *et al.*, "Joint Trajectory and Passive Beamforming Design for Secure UAV Networks with RIS," in *2020 IEEE Globecom Workshops (GC Wkshps*. IEEE, Dec. 7 2020, pp. 1–6.

[13] L. Yang *et al.*, "On the Performance of RIS-Assisted Dual-Hop UAV Communication Systems," *IEEE Trans. Veh. Technol*, vol. 69, no. 9, pp. 10 385–10 390, 2020.

[14] S. Li, B. Duo, M. Di Renzo, M. Tao, and X. Yuan, "Robust secure uav communications with the aid of reconfigurable intelligent surfaces," *IEEE Trans. Wirel. Commun*, vol. 20, no. 10, pp. 6402–6417, 2021.

[15] M. Abualhayja'a *et al.*, "Performance of reconfigurable intelligent surfaces vs. relaying for uav-assisted communications," in *2021 IEEE USNC-URSI Radio Science Meeting (Joint with AP-S Symposium)*. IEEE, Dec 4 2021, pp. 58–59.

[16] J. Hu and N. C. Beaulieu, "Accurate Closed-Form Approximations to Ricean Sum Distributions and Densities," *IEEE Wireless Commun. Lett.*, vol. 9, no. 2, pp. 133–135, 2005.

[17] Q. Wu *et al.*, "Intelligent Reflecting Surface-Aided Wireless Communications: A Tutorial," *IEEE Trans. Commun.*, vol. 69, no. 5, pp. 3313–3351, 2021.

[18] J. Marcum, "A statistical theory of target detection by pulsed radar," *IRE IEEE Trans. Inf. Theory*, vol. 6, no. 2, pp. 59–267, 1960.

[19] N. Temme, "Asymptotic and numerical aspects of the noncentral chi-square distribution," *Computers & Mathematics with Applications*, vol. 25, no. 5, pp. 55–63, 1993.

[20] A. M. Salhab and M. H. Samuh, "Accurate Performance Analysis of Reconfigurable Intelligent Surfaces Over Rician Fading Channels," *IEEE Wireless Commun. Lett.*, vol. 10, no. 5, pp. 1051–1055, 2021.

[21] S. Shimamoto *et al.*, "Channel Characterization and Performance Evaluation of Mobile Communication Employing Stratospheric Platforms," *IEICE Trans. Commun.*, vol. 89, no. 3, pp. 937–944, 2006.

[22] A. Al-Hourani, S. Kandeepan, and S. Lardner, "Optimal LAP Altitude for Maximum Coverage," *IEEE Wireless Commun. Lett.*, vol. 3, no. 6, pp. 569–572, 2014.